

Analyst

Accepted Manuscript



This is an *Accepted Manuscript*, which has been through the Royal Society of Chemistry peer review process and has been accepted for publication.

Accepted Manuscripts are published online shortly after acceptance, before technical editing, formatting and proof reading. Using this free service, authors can make their results available to the community, in citable form, before we publish the edited article. We will replace this *Accepted Manuscript* with the edited and formatted *Advance Article* as soon as it is available.

You can find more information about *Accepted Manuscripts* in the [Information for Authors](#).

Please note that technical editing may introduce minor changes to the text and/or graphics, which may alter content. The journal's standard [Terms & Conditions](#) and the [Ethical guidelines](#) still apply. In no event shall the Royal Society of Chemistry be held responsible for any errors or omissions in this *Accepted Manuscript* or any consequences arising from the use of any information it contains.

Cite this: DOI: 10.1039/c0xx00000x

www.rsc.org/xxxxxx

ARTICLE TYPE

Urinary Micro-RNA Biomarker Detection Using Capped Gold Nanoslit SPR in a Microfluidic Chip

Mansoureh Z. Mousavi,^a Huai-Yi Chen,^{a,b,e} Kuang-Li Lee,^{a,k} Heng Lin,^f Hsi-Hsien Chen,^{g,h} Yuh-Feng Lin,^{g,h} Wong Chung Shun,^{i,j} Hsiao Fen Li,^f Pei-Kuen Wei,^a Ji-Yen Cheng^{a,c,d,e,*}

Received (in XXX, XXX) Xth XXXXXXXXX 20XX, Accepted Xth XXXXXXXXX 20XX

DOI: 10.1039/b000000x

Successful diagnosis and treatment of many diseases depends on the availability of sensitive, reliable and low cost tools for the detection of the biomarkers associated with the diseases. Simple methods that use non-invasive biological samples are especially suitable for the deployment in clinical environment. In this paper we demonstrate the application of a method that employ capped gold nanoslit surface plasmon resonance (SPR) sensor and microfluidic chip for the detection of a urinary nucleic acid biomarker in clinical samples. This method detects low concentration biomarker in a relative large volume (~1mL) of sample. The method utilizes magnetic nanoparticles (MNPs) for the isolation of target molecule and signal enhancement in conjunction with surface plasmon resonance (SPR) on capped gold nanoslits. The ability of the method to detect urinary miRNA-16-5p in AKI patients was tested and the result was compared with the data obtained with polymerase chain reaction (PCR). miRNA-16-5p has been found to be a specific and noninvasive biomarker for acute kidney injury (AKI). Our method allows the detection of the biomarker in urine of AKI patients without amplification and labeling of the target molecules.

1. Introduction

Micro-ribonucleic acids (miRNA) have been used as diagnosis and prognosis biomarkers¹⁻³. Weber et al have shown the presence of miRNA in human fluids such as plasma, saliva, tears and urine and they have demonstrated the potential of these extracellular miRNAs in human fluids as biomarker for detection of physiopathological conditions⁴. With their high stability in body fluids, miRNAs are potential biomarkers for cancer diagnosis⁵. Detection of miRNA biomarkers in urine makes non-invasive diagnostic possible. However, the concentration of miRNA in urine, compare to those in other body fluids, is the lowest². Developing a sensitive method to detect miRNA in urine for non-invasive diagnosis of diseases is critical for the development of diagnosis devices for clinical application. Polymerase chain reaction (PCR) is one of the available techniques to detect miRNA in urine. However, PCR is a label based and multistep methods that usually require significant sample preparation and experienced personnel to conduct the test⁶.

Surface plasmon resonance (SPR) is one of the biosensor technologies with applications in medical diagnostics⁷⁻⁹. SPR-based sensors offer rapid, label-free detection methods with the ability to observe the kinetic reaction process in real time¹⁰. Compare to most commonly used, attenuated total internal reflection (ATR) sensors, SPR sensors based on gold nanostructures allow using probe light at normal incidence and facilitate chip-based integration and high-throughput and label-free detections of biomarkers. Sensitive periodic nanostructure

SPR with extraordinary optical transmission has being very promising for biosensing applications¹¹⁻¹⁵. In this work, highly sensitive capped gold nanoslit (CG nanoslit) film was used as the sensing platform.

Microfluidics, with the ability of fluid manipulation on the microscale, sample enrichment, isolation and sorting, provides applications in biological analysis. Microfluidic systems have been shown to be extremely useful and powerful for the preparation, delivery and analysis of samples, as well as cell sorting and separation. Integrating microfluidics with plasmonic sensors allows for the creation of a portable, stable and robust Lab-On-Chip system for label-free detection¹⁶⁻²⁴.

Previously, we developed a detection method that uses gold nanoslit SPR for detection of mRNA hnRNP B1, which is a promising biomarker in early stage of lung cancer²⁵. Such a sensitive detection technique that has integrated microfluidic chip has the potential of being developed into efficient and effective biosensing platforms. Unfortunately, the microfluidic chip used in the previous work is only capable of handling small volume of sample (~ 7 micro liters). However, to detect low concentrations of biomarker in urine, it is necessary to process volume of samples of the order of milliliters. In this paper we demonstrate a new design of microfluidic chip to integrate with the novel sensitive CG nanoslit film to detect low concentration of urinary miRNA biomarker.

In this work we demonstrate a label-free detection of rare miRNA in urine of patients with acute kidney injury (AKI). Presence of miRNA in urine has been reported as a biomarker for kidney injury^{26, 27}. Early stage diagnosis is very important for the

1 treatment of AKI. Current standard marker (serum Creatinine)
 2 does not reveal the injury until 48 to 72 hours, which is late for
 3 effective treatment. Lin *et al.* have shown that urinary miR-494
 4 expression levels are significantly higher only in AKI patients
 5 and the level increases significantly before the rise of serum
 6 creatinine level²⁸. Lin *et al.* have also discovered that miR-16-5p
 7 was found in urine of AKI patients and not in normal subjects
 8 (manuscript to be submitted). They suggested that urinary
 9 miRNA-16-5p can be served as a specific and noninvasive
 10 biomarker for AKI. Here, we focused on developing a method
 11 based on label-free nanostructure transmission SPR for detection
 12 of urinary miRNA-16-5p in early stage of AKI. In a close
 13 collaboration with physicians, urine samples from patients were
 14 tested with our method and the result were compared with PCR
 15 data.

17 2. Material and Methods

18 2.1. Materials

19 Fe_3O_4 MNPs modified with amino groups (TANBead[®] USPIO-
 20 101) with particle sizes of 6~10 nm and concentrations of 10
 21 mg/ml (1.4×10^{16} MNPs/ml) were purchased from Tanbead. The
 22 MNP surface was modified with a cross-linker, sulfosuccinimidyl
 23 4-(N-maleimidomethyl) cyclohexane-1-carboxylate (sulfo-
 24 SMCC, Thermo scientific Prod# 22322). The synthetic
 25 oligonucleotides were obtained from Proligo. The oligonucleotide
 26 sequences are listed in Table 1.

27 2.2. Double hybridization method

28 In this work, CG nanoslit SPR as sensing platform was employed
 29 to detect low concentration biomarker in urine. Similar to our
 30 previous work²⁵, a double hybridization method was applied to
 31 isolate and detect the target molecule. The approach includes
 32 double hybridization in two steps. As shown in figure 1, in the
 33 first step, functionalized iron oxide MNPs immobilized with the
 34 oligonucleotide probe complementary to the target sequence
 35 (probe I) isolates the target molecule from urine sample. MNPs
 36 were isolated and the supernatant was removed. The MNPs
 37 carrying the target molecules were re-suspended in hybridization
 38 buffer. In the second steps the isolated target molecule on the
 39 MNPs is allowed to hybridize with the second complementary
 40 probe (probe II) immobilized on the CG nanoslit (schematic
 41 figure 1). The concentration of MNPs must be optimized to
 42 obtain the maximum efficiency of the isolation. In the case of low
 43 concentration target molecule in large volume of sample,
 44 increasing the number of MNPs increases the probability of
 45 capturing. However, the concentration of the MNPs must be kept
 46 below a concentration to avoid SPR background noise due to the
 47 "Brownian motion" of the MNPs. The concentration of $\sim 1 \times 10^{13}$
 48 particles per 1 mL of urine was found to be the optimal value and
 49 was used for all experiments in this paper.

50 2.2.1 Designing two specific probes

51 Double hybridization at two different specific locations in the two
 52 steps results in a very specific nucleic acid detection method. The
 53 probe I and probe II sequences were designed based on the target
 54 molecule sequence. Probe I is a 23-mer oligonucleotide sequence
 55 that includes a 12-mer T spacer and a 11-mers sequence, which is
 56 complementary to the 12–22 region of miRNA-16-5p. The 5'-end
 57
 58
 59
 60

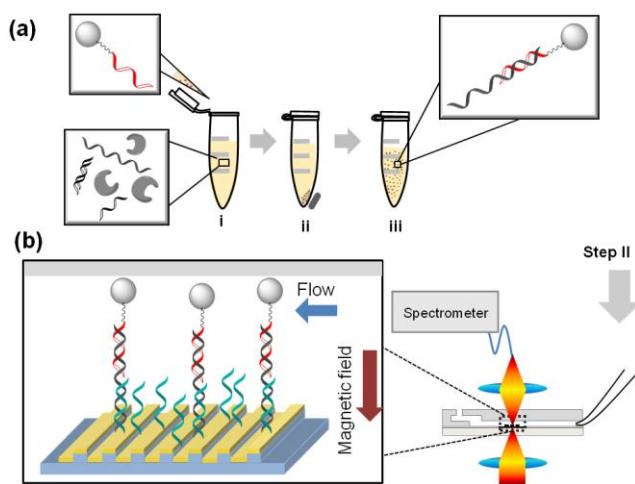


Figure 1 A schematic of the double hybridization method to detect the nucleic acid target (a) First step: isolation of the target molecule using MNPs (b) Second step: hybridizing the target molecule isolated on the MNPs with Probe II on the CG nanoslit.

of probe I is modified with a sulfhydryl group (C_6SH) to attach to the functionalized MNPs. Probe I on the MNPs hybridizes with the target molecule in the first step to isolate the target molecules in the urine sample to reduce the interference of non-target nucleic acids, proteins and possible cell debris on the second hybridization step. Probe II is a 23-mers oligonucleotide that includes a 12-mer T spacer and an 11-mer sequence complementary to the 1–11 region of miRNA-16-5p. The 3'-end of probe II is modified with a sulfhydryl group (C_3SH) to attach to the CG nanoslit surface. Probe II hybridizes with the target molecule isolated in the first step. The hybridization event in the second step is detected by the SPR method. Probes I and II are designed to be complementary to the unique region of the target miRNA-16-5p sequence. The sequences of probe I and probe II are shown in Table 1.

To detect a nucleic acid biomarker in a complex sample matrix such as urine and avoiding the non-specific binding of non-target molecule, the composition of hybridization solution needs to be optimized. We optimized the salt concentration (stringency) and formamide percentage to achieve high specific method to detect miRNA-16-5p in urine sample.

50 2.2.2 Functionalization of MNPs and CG nanoslit surface

Fifty microliters of the MNP suspension from a stock ($25 \mu\text{M}$) was suspended in 25 mL of $1 \times \text{PBS}$ buffer. Then, 25 mg of the cross-linker (sulfo- SMCC) was added, and the mixture was allowed to react overnight. Using a magnet, the modified MNPs were isolated and then re-suspended in $10 \mu\text{L}$ of $1 \times \text{PBS}$ buffer. One hundred microliter of a $100 \mu\text{M}$ solution of thiol-modified probe I was added to the tube and was allowed to react overnight. MNPs functionalized with Probe I were then separated with a magnet, washed and re-suspended in 8 mL of $1 \times \text{PBS}$ buffer. The suspension of the probe I immobilized MNPs can be stored in a 4°C for up to one month. This batch of probe-I-immobilized-MNP can be used for 20 detections. For each detection, $400 \mu\text{L}$ of the probe-I-immobilized-MNP is used.

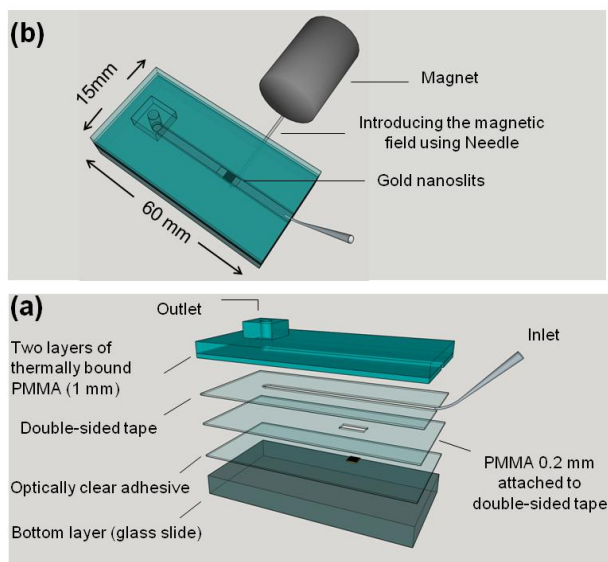


Figure 2 (a) top view of the funnel chip integrated with CG nanoslit film and the magnet. The needle was used to introduce the magnetic field to the detection area. (b) Layered structure of the microfluidic chip integrated with a CG nanoslit film.

The CG nanoslit film was integrated with the microfluidic chip and the surface of CG nanoslits was functionalized by immobilizing the complementary probe II. A solution of 10 μM thiol-modified probe II was introduced to the funnel chip. The CG nanoslit surface was allowed to react with probe II for overnight and was then rinsed twice with 1 \times PBS buffer (the buffer was flowed to the channel of funnel chip). The CG nanoslit functionalized with probe II can be stored at 4 $^{\circ}\text{C}$ up to one month before the SPR measurement.

2.3. A novel microfluidic chip to process large volume of sample

Microfluidic systems, as an emerging technology in clinical applications, provide various advantages including process integration and short analysis time. Detection of low concentration biomarker requires processing a large volume of sample. A novel fluidic chip, funnel chip, for introducing large volume of sample was designed and fabricated to integrate with the CG nanoslit film for detection of rare miRNA biomarker in the urine sample. The structure of funnel chip is shown in Figure 2.

The microfluidic chips were fabricated using a laser scribe to ablate trenches on polymethylmethacrylate (PMMA) substrates and double-sided tape^{29, 30}. The PMMA substrates were then bonded together by thermal binding and with the CG nanoslit film using the double-sided tapes. The gold nanoslit film integrated with PMMA layers was then attached to a glass slide using an optically clear adhesive layer (3MTM optically clear adhesive 8263). A gel loading pipet tip (Labcon, Cat# 1034-800-000) was used as the sample reservoir and the connector to introduce the sample to the microchannel accommodating the SPR sensor. A Nickel-coated ferritic iron needle attached to a cylindrical neodymium magnet was put beneath the nanoslit to bring the MNPs carrying the target to the surface to bind with the

probe II immobilized on the gold nanoslits. This design provides an efficient way to capture target molecule with minimal non-specific binding due to shear forces produced by fluid flow. Furthermore, integrating a magnet to the microfluidic chip to bring the MNPs carrying the target molecule to the SPR sensor surface improves the efficiency of capturing.

2.4. Fabrication of CG nanoslits

In this work, CG nanoslit platform developed by Lee. et al. was employed as the sensing platform. The CG nanoslit film consist of an upper layer of periodic metallic nanowires and a lower layer of periodic metallic nanoslits. The period of both layers is 600 nm. The CG nanoslit were fabricated on a 178- μm -thick cyclic olefin polymer (COP) film using nanoimprint lithography. The development of CG nanoslit sensing platform has been described in Lee et. al.³¹. Briefly, the CG nanoslit film was fabricated as follow. First, nanogrooves of 80 nm in width and 80 nm in depth on a silicon substrate were fabricated using electron beam lithography and a reactive ion etching method. A 300-nm-thick ZEP-520 resist (ZEP-520, Zeon Corp, Tokyo, Japan) was spin-coated on a 525- μm -thick silicon substrate. An electron-beam writing system (Elionix ELS 7000) was used to write groove arrays. The patterns were then transferred to the silicon substrate by using a reactive ion etching machine (Oxford Instrument, plasmalab 80plus). The silicon template and COP film were placed on a heating plate and heated to a temperature of 170 $^{\circ}\text{C}$ to soften the polymer substrate. The template and substrate were cooled before removal from the chamber. The COP film now bearing periodic nanoridges was then peeled off the template. Finally, sputtering an 80-nm-thick gold film on the imprinted plastic substrate completed the fabrication of the CG nanoslit film.

2.5. Urine sample

Human serum and urine samples were obtained from 2 critical patients who developed AKI, defined as ≥ 1.5 -fold increase in serum creatinine, in compliance with Acute Kidney Injury Network criteria. Patients were admitted to the Department of Internal Medicine, Taipei Medical University Hospital (Taipei, Taiwan) and Tzu Chi General Hospital (Hualien Taiwan). This research project was approved by the Institutional Review Board of the Department of Internal Medicine, Taipei Medical University Hospital, and informed consents were obtained from all patients. Urine samples were obtained from 6 healthy volunteers as well. All samples were frozen at -80 $^{\circ}\text{C}$ until use. The sample of urine (1 mL) was thawed at room temperature prior to the detection of the target miRNA by the double hybridization method. The suspension of the functionalized MNPs (final concentration 2×10^{13} particles per mL) and hybridization buffer (final concentration of 1 \times SSC solution, 7.5% of formamide) were mixed with the urine sample in an Eppendorf tube and allowed to hybridize for one hour at room temperature. By using a magnet, MNPs were isolated and the supernatant was removed. The MNPs carrying the target molecules were re-suspended in 150 μL of hybridization buffer (final concentration of 9 \times SSC solution, 30% of formamide). Following the first step, the MNPs suspension was introduced to the funnel chip to hybridize with probe II on the CG nanoslit.

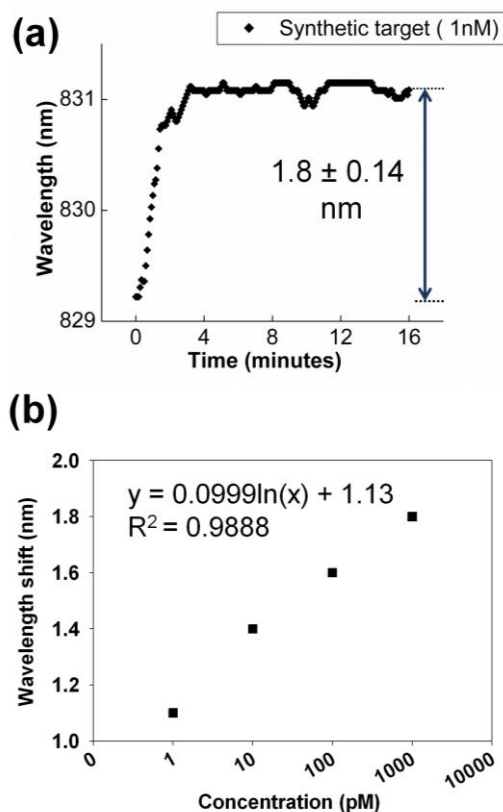


Figure 3 (a) The dynamic SPR response that indicates the real-time progression of the hybridization of target molecule with the probe II on the CG nanoslit, (b) The calibration curve obtained for various concentration of synthetic miRNA-16-5p spiked in urine from healthy subjects

2.6. SPR measurement

A transverse magnetic-polarized wave in the CG nanoslit generated sharp and asymmetric Fano resonances in transmission spectra. Surface plasmon resonance of the fabricated CG nanoslits with a period of 600 nm manifested as a transmission spectrum in a wavelength range of 820-850 nm when the hybridization buffer is put in contact with the nanoslit film. The position of the SPR spectrum shifts due to the environmental changes around the nanoslits. The hybridization of the immobilized probe II on the CG nanoslit and the target molecule leads to a red shift in the SPR resonance wavelength. The SPR response was recorded every 5 seconds during the hybridization reaction. The measurement started 30 seconds after introducing the sample. Raw data were obtained and processed with a home-written MATLAB® program. The wavelength at the local minimum of the SPR spectrum was identified by applying a local maximum-minimum method. (Koptenko 2003, available on <http://www.mathworks.com/matlabcentral/fileexchange/3170>). The wavelength at the local minimum of the SPR spectrum was plotted against time. The resulting graph indicates the real-time progression of the hybridization reaction.

2.7 RNA Isolation

The human urine RNA was extracted using the QiAMP

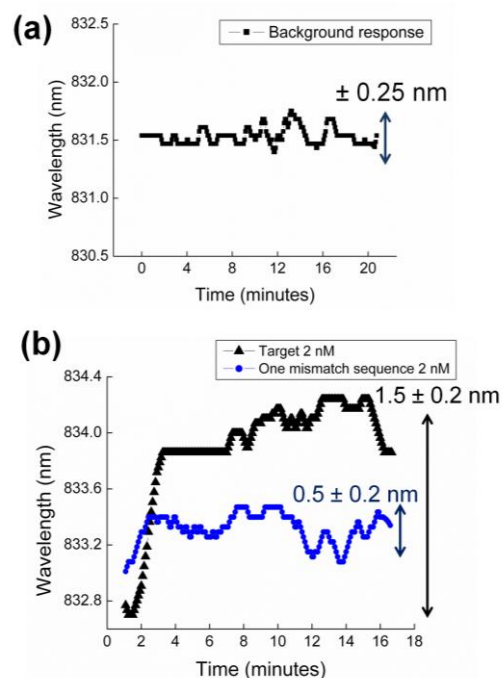


Figure 4 (a) The dynamic SPR response from applying the method to a blank sample (b) The dynamic SPR response from applying the method to a sample of 2 nM one mismatch sequence in comparison with the response from a sample of 2 nM perfect match sequence

circulating nucleic acid kit (Qiagen). RNA isolation was performed according to the manufacturer's instructions.

2.8 Quantitative PCR and reverse transcription PCR

The ABI PRISM 7700 Sequence Detection System (ABI) was used for quantitative PCR (Q-PCR) analysis. For the detection of miR-16-5p expression, stem-loop Q-PCR was carried out using the TaqMan miRNA Assays with TaqMan® Universal Master Mix II according to standard procedure (Life Technologies, CA, USA). Q-PCR was performed using the TaqMan 2 × universal master mix and 20× TaqMan miRNA assay (primers & probe). All samples were run in duplicate and the resulting C_t values averaged. Relative expression was evaluated by the comparative threshold cycle method. The expression of miRNA-16-5p was normalized to the expression of U6 small nuclear RNA (U6 snRNA), which is commonly used as a reference gene in miRNA quantification.

3. RESULT and DISCUSSION

3.1. Detection of biomarker in large volume of sample

Previously we have demonstrated a novel platform for detecting nucleic acid biomarkers in small volumes of sample. However, the microfluidic device needs to be re-designed in order to handle large sample volume. The performance of a biosensor is limited by the efficiency at which the analyte can be brought into proximity of the sensing element to bind with the recognition molecules on the sensor surface^{32,33}.

In most surface-based sensors such as SPR, interaction between

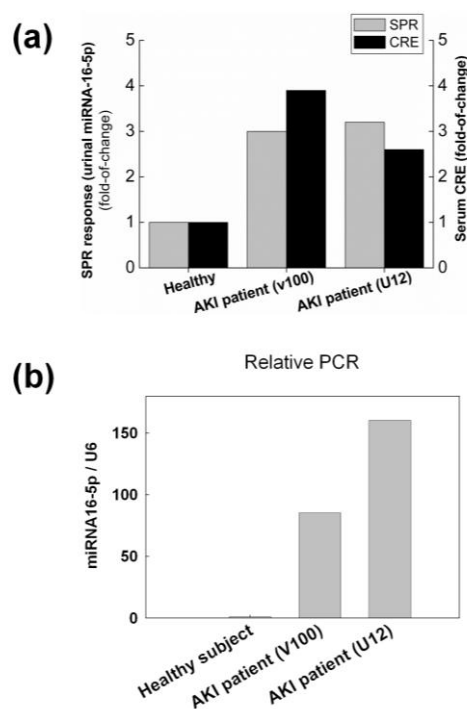


Figure 5 a) The double hybridization method to detect miRNA-16-5p was applied to two AKI patients and healthy subjects. The graph shows the fold-of-change of SPR response of two AKI patients (left Y axis). For comparison the right Y axis shows the fold-of-change in serum Creatinine (CRE) of AKI patients. (b) Relative expression of urinary miRNA-16 of the two AKI patients obtained with PCR

the analyte and the recognition probe is limited by diffusion. Mass transfer to the reactive surfaces, the saturation time scales and the capture fractions in flow are important parameters that require being optimized³⁴.

When the recognition process is limited only by diffusion, the detection limit is determined by analyte mass transport³⁵. Ways to improve this aspect are highly desirable to improve the performance of a biosensor. Here, in this work, we fabricated a microfluidic chip with integrated magnet to maximize interactions between the target molecule and the probe on the CG nanoslit while the liquid flow minimizes the non-target interference. In this way we can improve the biosensor performance to detect a biomarker in large volume of samples.

3.1.2.1 Optimization of the flow velocity

We designed a microfluidic chip to flow the suspension of MNPs-target to bind with the second complementary probe on the CG nanoslit. The velocity of the flow has been optimized to achieve the high efficiency of detection. Maximum sensitivity and lowest detection limit was achieved when the suspension of the MNPs carrying the target was introduced to the funnel chip with the flow rate of 6 $\mu\text{L}/\text{min}$. The corresponding laminar shear is only 0.006 Dyne/cm². The following equation was used to

calculate the laminar shear³⁶.

$$\tau = \frac{6\mu Q}{wh^2}$$

Where τ is the strength of laminar shear stress in the unit of Dyne/cm² (1 Pascal =10 Dyne/cm², and μ is the dynamic viscosity of the solution (for PBS is 1.0 cP or 0.001 Pa.s)³⁷, Q is the velocity of flowing rate (0.0001 cm³/s) and W is the width (0.1 cm) and h is the height (0.1 cm) of flow channel.

3.2. Detection of Synthetic miRNA-16-5p spiked in urine of healthy subjects

The sensitivity of the method was evaluated by detecting the synthetic target molecule spiked in 1 mL of urine sample from healthy subject. Figure 3 (a) shows the dynamic SPR response when the double hybridization method was applied to a 1 nM solution of synthetic target molecule representing miRNA-16-5p. A calibration curve (figure 3(b)) was obtained from the values of the shifts in the wavelength of SPR resonance for various concentrations of the target molecule. The equation of ($y = 0.0999\ln(x) + 1.13$), $R^2 = 0.9888$) was obtained for the calibration curve.

The reference response was obtained when the double hybridization method was applied to a urine sample of healthy subjects without adding the synthetic target (blank). The dynamic SPR response for the blank sample is shown in figure 4 (a). A slight signal fluctuation due to the Brownian motion was observed. The standard deviation of the SPR response fluctuation was 0.25 nm, which is considered as the background noise. The detection limit of the method is the concentration at which the shift of the SPR spectrum position is 0.75 nm (i.e. three times STD). Inserting this number in the equation yields the detection limit of 17 fM. Detection of target molecule in a range from tens of femtomolar to nanomolar makes this method suitable for detection of AKI.

3.3. Specificity assessment by detection of single nucleotide mismatch

To evaluate the specificity of the method, a high concentration solution of a one mismatch sequence was used as sample (the nucleotide sequence of the one mismatch molecule is shown in Table 1). Double hybridization method was applied to a sample of 2 nM solution of one mismatch sequence. A 0.5 ± 0.2 nm shift in the wavelength of SPR spectrum position was observed. The dynamic SPR response for the one mismatch sequence is shown in Figure 4(b). Comparing the responses confirm the high specificity of our method. Mismatched sequence was clearly distinguishable from the fully matched complementary target. The high specificity is the result of pre-isolation of target molecule, double hybridization and optimized flow of sample to minimize the non-specific binding of non-target molecules. SPR has been reported as a sensitive method for detection of oligonucleotide mismatches^{38,39}.

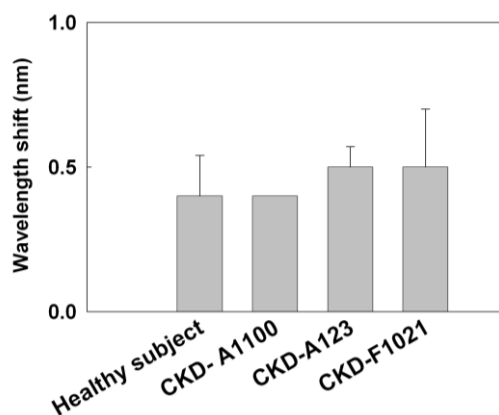


Figure 6 The values of SPR wavelength shift when applying the method to 1 mL of urine from three CKD patients. The data are expressed as means \pm SD of two measurements for CKD-A123 and CKD-F1021.

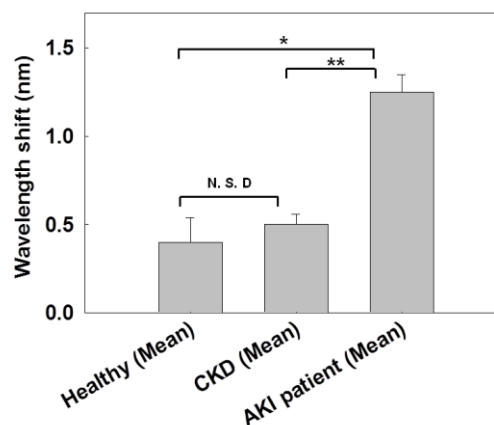


Figure 7 Comparing the SPR responses when double hybridization method was applied to healthy, CKD and AKI subjects. The data are expressed as means \pm SD. * $P < 0.05$, ** $P < 0.01$. N.S.D, no significant difference.

3.4. Detection of miRNA-16-5p in urine of AKI patient

Double hybridization method was applied to detect urinary miRNA-16-5p of AKI patients. Urine samples of two AKI patients were received from the hospital. Urine from six healthy donors was mixed and used as the healthy subject in this test. Figure 5(a) shows the fold-of-change of SPR response detecting urinary miRNA-16-5p of two AKI patients compare to the healthy subject (left Y axis). For comparison, the right Y axis shows the fold-of-change in serum Creatinine (CRE) of AKI patients. The serum CRE values for AKI patients were provided by the hospital. The average of CRE values reported in previous studies⁴⁰ was used as reference for healthy patients.

Furthermore, our result was compared with the result of relative Q-PCR (figure 5(b)) to evaluate the capability of our method to detect miRNA in urine sample. A good agreement between SPR and PCR result to detect the presence of elevated level of miRNA-16-5p was confirmed. The results for the detection of miRNA-16-5p from patient's urine using the "double hybridization method" demonstrate a sensitive method for clinical application.

3.5. Distinguishing AKI from Chronic kidney disease

Further specificity test was carried out by applying the double hybridization method on patients with chronic kidney disease (CKD). Double hybridization method designed with probes to detect miRNA-16-5p was applied to CKD samples. This test was aimed to evaluate the specificity of our method to discriminate between AKI patients and CKD subjects. The SPR responses from applying the double hybridization method to 1 mL of urine from three CKD patients are shown in figure 6.

The comparison of SPR response when double hybridization method was applied to urine samples from healthy subjects, CKD and AKI patients are demonstrated in figure 7. Compared to the healthy and the CKD subjects, the SPR response for AKI patients were statistically significant ($p < 0.05$). There was no significant difference between the SPR responses of healthy and CKD subjects ($p = 0.6$). As it was mentioned above, we found a good

agreement between SPR and the relative Q-PCR results to detect the presence of elevated level of miRNA-16-5p. There are several limitations to use PCR for clinical applications. One of the limitations of PCR is the amount of time needed for sample preparation. Especially for RNA samples which requires a reverse-transcription step to convert the RNA molecules into DNA. Moreover, reverse-transcription step can be affected by the presence of inhibitors for reverse transcription enzymes that can leads to false-negative results⁴¹. Another limitation of PCR for clinical application is the multiplexing. Due to the temperature control and speed of amplification for different targets, multiplex analysis of number of target molecules is rather challenging. In comparison with label based and multi-steps PCR method, our method offers label-free, fast detection of analyte in a robust and simple platform which can be operated with minimal training. This, coupled with its low cost and ease of integration in a portable system, makes it an outstanding candidate for developing a clinically viable diagnostic tool for diseases such as AKI. We are now developing a portable system for rapid and reliable diagnosis of AKI.

4. Conclusions

In this paper we demonstrated a novel method for detection of miRNA-16-5p in urine as a promising method for rapid and non-invasive diagnosis of AKI. Our method is based on nanostructured transmission SPR integrated in microfluidic system for the introduction of the sample. The viability of our method for clinical application was evaluated by detecting the miRNA-16-5p biomarker in urine samples from patients with AKI. The results were compared with the established technique, PCR. Having confirmed the validity of this method for clinical application, further work will be focused on developing a portable system which can be deployed in clinical environments.

Our group has discovered seven miRNAs in urine of AKI patients that cannot be found in urine of healthy subjects. Using an array of CG nanoslit sensors, we are currently developing a platform

1 for simultaneous, multiplexed detection of seven AKI
2 biomarkers, with the aim of improving the sensitivity and
3 specificity of diagnosis.
4

5 **Acknowledgements**

6
7 5 This work is financially supported by the National Science
8 Council, Taiwan (Contract no. MOST 103-2113-M-001-003-
9 MY2) and the Focus group project of Research Center for
10 Applied Sciences, Academia Sinica, Taiwan. Technical support
11 from NanoCore, the core facilities for nanoscience and
12 10 nanotechnology at Academia Sinica in Taiwan, is acknowledged.
13
14
15
16
17
18
19
20
21
22
23
24
25
26
27
28
29
30
31
32
33
34
35
36
37
38
39
40
41
42
43
44
45
46
47
48
49
50
51
52
53
54
55
56
57
58
59
60

Table 1

Oligonucleotide	Sequence (5' → 3')	Modification
Probe I ¹	TTTTTTTTTTTTTCGCCAATATTT	5' modification (C ₆ SH)
Probe II ²	ACGTGCTGCTATTTTTTTTTTTT	3' modification (C ₃ SH)
Target ³	TAGCAGCACGTAAATATTGGCG	None
Single mismatch ⁴	TAGCAGCACGTAAATACTGGCG	None

1- Complementary sequence to the region of 12-22 of miRNA 16-5p

2- Complementary sequence to the region of 1-11 of miRNA 16-5p

3- miRNA 16-5p sequence

4- Single nucleotide mismatch sequence

Notes and references

^a Research Center for Applied Sciences, Academia Sinica, Taiwan

^b Department of Engineering and System Science, National Tsing Hua University, Taiwan

^c Institute of Biophotonics, National Yang-Ming University, Taipei, Taiwan

^d Department of Mechanical and Mechatronic Engineering, National Taiwan Ocean University, Taiwan

^e Nano Science and Technology Program, Taiwan International Graduate Program, Academia Sinica and National Tsing Hua University, Taiwan

^f Department of Physiology, School of Medicine, College of Medicine, Taipei Medical University, Taipei, Taiwan

^g Department of Internal Medicine, School of Medicine, College of Medicine, Taipei Medical University, Taipei, Taiwan.

^h Division of Nephrology, Department of Internal Medicine, Taipei Medical University Hospital, Taipei, Taiwan.

ⁱ Graduate Institute of Clinical Medicine, College of Medicine, Taipei Medical University, Taiwan

^j Department of Emergency Medicine, Taipei Medical University-Shuang Ho Hospital, Taipei, Taiwan

^k Institute of Physics, Academia Sinica, Taiwan

* Corresponding author, E-mail: jycheng@gate.sinica.edu.tw

25

- 1 J. Lu, G. Getz, E. A. Miska, E. Alvarez-Saavedra, J. Lamb, D. Peck, A. Sweet-Cordero, B. L. Ebert, R. H. Mak, A. A. Ferrando, J. R. Downing, T. Jacks, H. R. Horvitz and T. R. Golub, *Nature*, 2005, **435**, 834-838.
- 2 H. Mlcochova, R. Hezova, M. Stanik and O. Slaby, *Urologic Oncology: Seminars and Original Investigations*, 2014, **32**, 41.e41-41.e49.
- 3 J. B. Li, S. B. Tan, R. Kooger, C. Y. Zhang and Y. Zhang, *Chem. Soc. Rev.*, 2014, **43**, 506-517.
- 4 J. A. Weber, D. H. Baxter, S. L. Zhang, D. Y. Huang, K. H. Huang, M. J. Lee, D. J. Galas and K. Wang, *Clin. Chem.*, 2010, **56**, 1733-1741.
- 5 N. Kosaka, H. Iguchi and T. Ochiya, *Cancer Sci.*, 2010, **101**, 2087-2092.
- 6 J. B. Weiss, *Clin. Microbiol. Rev.*, 1995, **8**, 113-130.
- 7 H. R. Jang, A. W. Wark, S. H. Baek, B. H. Chung and H. J. Lee, *Anal. Chem.*, 2014, **86**, 814-819.
- 8 T. Riedel, C. Rodriguez-Emmenegger, A. de los Santos Pereira, A. Bedajankova, P. Jinoch, P. M. Boltovets and E. Brynda, *Biosens. Bioelectron.*, 2014, **55**, 278-284.
- 9 L. C. Su, Y. C. Tian, Y. F. Chang, C. Chou and C. S. Lai, *J. Biomed. Opt.*, 2014, **19**, 6.
- 10 J. Homola, *Anal. Bioanal. Chem.*, 2003, **377**, 528-539.
- 11 A. Lesuffleur, H. Im, N. C. Lindquist and S.-H. Oh, *Applied Physics Letters*, 2007, **90**, -.
- 12 K. L. Lee, S. H. Wu and P. K. Wei, *Opt. Express*, 2009, **17**, 23104-23113.
- 13 K. L. Lee, W. S. Wang and P. K. Wei, *Plasmonics*, 2008, **3**, 119-125.
- 14 K. L. Lee, W. S. Wang and P. K. Wei, *Biosens. Bioelectron.*, 2008, **24**, 210-215.
- 15 K. L. Lee, P. W. Chen, S. H. Wu, J. B. Huang, S. Y. Yang and P. K. Wei, *ACS Nano*, 2012, **6**, 2931-2939.
- 16 C. D. Chin, V. Linder and S. K. Sia, *Lab Chip*, 2007, **7**, 41-57.
- 17 F. B. Myers and L. P. Lee, *Lab Chip*, 2008, **8**, 2015-2031.
- 18 P. S. Dittrich and A. Manz, *Nat. Rev. Drug Discov.*, 2006, **5**, 210-218.
- 19 S. Q. Wang, F. Inci, T. L. Chaunzwa, A. Ramanujam, A. Vasudevan, S. Subramanian, A. C. F. Ip, B. Sridharan, U. A. Gurkan and U. Demirci, *Int. J. Nanomed.*, 2012, **7**, 2591-2600.
- 20 A. Ozcan and U. Demirci, *Lab Chip*, 2008, **8**, 98-106.
- 21 Y. Wan, J. F. Tan, W. Asghar, Y. T. Kim, Y. L. Liu and S. M. Iqbal, *J. Phys. Chem. B*, 2011, **115**, 13891-13896.
- 22 O. Tokel, F. Inci and U. Demirci, *Chem. Rev.*, 2014, **114**, 5728-5752.
- 23 C. D. Chin, T. Laksanasopin, Y. K. Cheung, D. Steinmiller, V. Linder, H. Parsa, J. Wang, H. Moore, R. Rouse, G. Umvilijhozo, E. Karita, L. Mwambarangwe, S. L. Braunstein, J. van de Wijgert, R. Sahabo, J. E. Justman, W. El-Sadr and S. K. Sia, *Nat Med*, 2011, **17**, 1015-1019.
- 24 B. V. Chikkaveeraiah, V. Mani, V. Patel, J. S. Gutkind and J. F. Rusling, *Biosensors and Bioelectronics*, 2011, **26**, 4477-4483.
- 25 M. Z. Mousavi, H. Y. Chen, S. H. Wu, S. W. Peng, K. L. Lee, P. K. Wei and J. Y. Cheng, *Analyst*, 2013, **138**, 2740-2748.
- 26 E. Aguado-Fraile, E. Ramos, E. Conde, M. Rodriguez, F. Liano and M. L. Garcia-Bermejo, *Nefrologia*, 2013, **33**, 826-834.
- 27 N. Wang, Y. Zhou, L. Jiang, D. H. Li, J. W. Yang, C. Y. Zhang and K. Zen, *PLoS One*, 2012, **7**, 8.
- 28 Y. F. Lan, H. H. Chen, P. F. Lai, C. F. Cheng, Y. T. Huang, Y. C. Lee, T. W. Chen and H. Lin, *J. Am. Soc. Nephrol.*, 2012, **23**, 2012-2023.
- 29 J. Y. Cheng, C. W. Wei, K. H. Hsu and T. H. Young, *Sens. Actuator B-Chem.*, 2004, **99**, 186-196.
- 30 J. Y. Cheng, M. H. Yen, C. T. Kuo and T. H. Young, *Biomicrofluidics*, 2008, **2**, 12.
- 31 K.-L. Lee, J.-B. Huang, J.-W. Chang, S.-H. Wu and P.-K. Wei, *Sci. Rep.*, 2015, **5**.
- 32 P. R. Nair and M. A. Alam, *Applied Physics Letters*, 2006, **88**, 3.
- 33 P. E. Sheehan and L. J. Whitman, *Nano Lett.*, 2005, **5**, 803-807.
- 34 T. Gervais and K. F. Jensen, *Chem. Eng. Sci.*, 2006, **61**, 1102-1121.
- 35 W. T. Hsu, W. H. Hsieh, S. F. Cheng, C. P. Jen, C. C. Wu, C. H. Li, C. Y. Lee, W. Y. Li, L. K. Chau, C. Y. Chiang and S. R. Lyu, *Anal. Chim. Acta*, 2011, **697**, 75-82.
- 36 S. H. Wu, K. L. Lee, R. H. Weng, Z. X. Zheng, A. Chiou and P. K. Wei, *PLoS One*, 2014, **9**, 8.
- 37 F. Momen-Heravi, L. Balaj, S. Alian, A. J. Trachtenberg, F. H. Hochberg, J. Skog and W. P. Kuo, *Frontiers in Physiology*, 2012, **3**.
- 38 L. G. Carrascosa, A. Calle and L. M. Lechuga, *Anal. Bioanal. Chem.*, 2009, **393**, 1173-1182.
- 39 E. Milkani, S. Morais, C. R. Lambert and W. G. McGimpsey, *Biosens. Bioelectron.*, 2010, **25**, 1217-1220.
- 40 H. Finney, D. J. Newman and C. P. Price, *Ann. Clin. Biochem.*, 2000, **37**, 49-59.
- 41 C. Schrader, A. Schielke, L. Ellerbroek and R. Johne, *J. Appl. Microbiol.*, 2012, **113**, 1014-1026.